Chinese Journal of Chemical Engineering 95 (2026) 139–150

Contents lists available at ScienceDirect

Chinese Journal of Chemical Engineering

journal homepage: www.elsevier.com/locate/CJChE

Full Length Article

Controllable self-biodegradation of polycaprolactone/polyurethane composite sutures enabled by random heteropolymers-immobilized lipase

Jianqi Lu [1, 2], Lingling Fan [1, 2], Yihu Wang [1, 2], Xiaoli Zhou [1, 2, *], Yujia Peng [1, 2, *], Weiliang Dong [1, 2], Min Jiang [1, 2, 3]

[1] *Key Laboratory for Waste Plastics Biocatalytic Degradation and Recycling, College of Biotechnology and Pharmaceutical Engineering, Nanjing Tech University, Nanjing 211816, China*
[2] *State Key Laboratory of Materials–Oriented Chemical Engineering, Nanjing Tech University, Nanjing 211816, China*
[3] *Jiangsu National Synergetic Innovation Center for Advanced Materials (SICAM), Nanjing Tech University, Nanjing 211816, China*

ARTICLE INFO

Article history:
Received 16 September 2025
Received in revised form
15 January 2026
Accepted 1 February 2026
Available online 3 April 2026

Keywords:
Biodegradation
PCL/PU
Sutures
Composites
Polymers
Enzyme

ABSTRACT

Current absorbable sutures face challenges in matching heterogeneous tissue healing timelines, leading to postoperative complications from delayed degradation. Thus, self-biodegradable polycaprolactone/polyurethane (PCL/PU) composite sutures *via* electrospinning, incorporating *Burkholderia cepacia* lipase (BCL) stabilized by random heteropolymers (RHP) was developed in this research. RHP can maintain BCL activity retention at 40%–90% in organic solvents. The PCL70/PU30 suture exhibited optimal mechanics (tensile strength was (28.44 ± 1.25) MPa and Young's modulus was (42.43 ± 5.3) MPa), following the incorporation of the BCL-RHP complex, the suture's key mechanical properties were largely maintained and remained within the range compatible with typical suture applications. Enzyme-loading gradients (0.05%–0.5% (mass)) enabled precise degradation control. 0.5% (mass) enzyme-loaded sutures fully disintegrated spontaneously in simulated wound fluid within 15 days, this timeframe aligns with the typical epidermal healing cycle (approximately 2 weeks), suggesting the potential for achieving dynamic degradation-healing synchronization *in vivo*. In addition, functionalization of self-biodegradable composite sutures was achieved by embedding thymol for synergistic bioactivity. Thymol achieved a cumulative release of 86.76% ± 1.34% over 120 h, endowing the self-biodegradable composite sutures with sustained antioxidant (79.85% $ABTS^{+}$ scavenging rate) and antibacterial activity (significantly suppressing the growth of *Staphylococcus aureus*). Concurrently, the self-biodegradable composite sutures demonstrated favorable cytocompatibility in L929 fibroblast cell. The RHP-enabled enzyme stabilization strategy overcomes clinical-ecological limitations of conventional sutures, offering programmable degradation and multifunctionality for precision medicine.
© 2026 The Chemical Industry and Engineering Society of China, and Chemical Industry Press Co., Ltd. All rights are reserved, including those for text and data mining, AI training, and similar technologies.

1. Introduction

As critical consumables in surgical interventions, global demand for sutures escalates annually by millions of dollars due to trauma management and medical procedures. This expanding market faces a transformative shift driven by precision medicine: Retrospective clinical analyses have established that delayed suture degradation is a direct cause of 32% of postoperative complications, including surgical site infections and granuloma formation [1]. This challenge is exacerbated in tissues with divergent healing timelines (*e.g.*, epidermis, 7–14 days, *versus* cartilage, 90–180 days) [2,3]. The homogeneous degradation profile (>60 days) of current absorbable sutures fails to accommodate such disparity, proving particularly inadequate in chronic wounds like diabetic foot ulcers and dynamic sites like cardiovascular stent fixation [2,4,5], where prolonged foreign body retention elevates reoperation rates by 18%–25% [6–8]. Consequently, therapeutic refinement drives innovation toward multifunctional and stimuli–responsive sutures [9–11].

Concurrently, rapid advancements in biomedical engineering necessitate synthetic polymers with enhanced biocompatibility

* Corresponding authors.
E-mail addresses: xlzhou@njtech.edu.cn (X. Zhou), yujia_peng@njtech.edu.cn (Y. Peng).

https://doi.org/10.1016/j.cjche.2026.02.006
1004-9541/© 2026 The Chemical Industry and Engineering Society of China, and Chemical Industry Press Co., Ltd. All rights are reserved, including those for text and data mining, AI training, and similar technologies.

and multifunctionality. This demand has spurred exploration into FDA-approved polymers-including polycaprolactone (PCL), poly(-methyl methacrylate) (PMMA), poly(lactic-*co*-glycolic acid) (PLGA), and polyurethane (PU)-focusing on their biological adaptation and tissue regeneration potential [12]. Owing to its exceptiona_mechanical strength and biocompatibility, PU is widely used in biomedical applications [13]. When used as suture material, it meets the specific mechanical requirements for high strength, high elasticity, and minimally invasive closure needed in dynamic physiological environments [14]. It is important to note that the mechanical requirements for sutures differ fundamentally from those for skin scaffolds used in tissue regeneration: the core function of sutures is to provide high tensile strength over the short term (days to weeks) to securely close wounds, making their mechanical properties (such as tensile strength) critical [15]. Skin scaffolds, on the other hand, focus on providing a three-dimensional porous structure over extended periods (weeks to months) to support cell migration, growth, and tissue regeneration. Their mechanical properties are designed to better match soft tissue characteristics and enhance bio-guidance [16] whereas PCL provides complementary advantages through tunable degradation kinetics and reinforced mechanical properties. Their synergistic integration enables biomimetic systems that closely replicate physiological microenvironments [17–19], rendering them particularly valuable for vascular grafts and dynamic tissue scaffolds. Nevertheless, conventional biodegradable polymers remain ecologically problematic due to two inherent limitations: (1) environmentally insensitive degradation leading to delayed decomposition, and (2) incomplete breakdown generating persistent microplastic pollution [20]. Thus, transcending degradation constraints through precisely controllable decomposition behavior represents a critical pathway toward resolving these global ecological and clinical challenges.

Self-biodegradable living plastics, serving as a emerging class of environmentally responsive materials, incorporate bioactive components (such as microbial spores or enzyme preparations) into the polymer matrix, which enables spontaneous degradation upon triggering by specific environmental signals. However, spore germination requires precise induction mechanisms, and the released active cells should efficiently express the target degradation enzymes. These requirements imposing higher demands on the genetic modification of host strains [21]. In contrast, enzymatic degradation pathways avoid byproduct generation *via* specific reactions and simplify downstream recovery. The enzyme embedding strategy, bypasses the need for complex spore germination regulation, enabling immediate triggering of the degradation process [22]. By uniformly dispersing polylactic acid (PLA) hydrolase into PLA *via* melt extrusion, the material can achieve complete decomposition within 20–24 weeks under home composting conditions [23]. PCL/lipase composite films fabricated by 3D printing technology undergo complete degradation after 7 days at 37 °C [24]. Nevertheless, these systems rely on the intrinsic thermal stability of enzymes. When material processing involves organic solvents (*e.g.*, hexafluoroisopropanol, chloroform), direct embedding of free enzymes into the material becomes unfeasible. Addressing this limitation, researchers at the University of California developed a random heteropolymers (RHP) as enzyme protectants, which form a protective layer around enzymes *via in-situ* encapsulation [25]. This strategy significantly enhances enzyme activity retention under harsh processing conditions, achieving 85% retention in melt extrusion and 92% in solvent casting [23]. In our prior research, the enzyme-loaded (*Burkholderia cepacia* lipase, BCL) PCL nanofiber scaffolds fabricated *via* electrospinning. This scaffold demonstrated complete degradation within 12–72 h while promoting scarless wound healing [16]. This RHP-based enzyme immobilization strategy applied to high-performance PCL/PU composite sutures also offers distinct advantages. First, RHP protection ensures enzyme activity in organic solvent spinning solutions, enabling the integrated preparation of enzyme–loaded sutures *via* electrospinning. Second, the suture's mechanical strength effectively stabilizes wounds, reducing healing delays caused by wound dehiscence [26]. Furthermore, by regulating the enzyme loading (*e.g.*, BCL at 0.05%–0.5% of total polymer mass), the degradation timeline of the suture can be precisely programmed (ranging from hours to weeks). This allows matching the healing time windows of different tissues, thereby reducing the need for suture removal [27]. Finally, this strategy overcomes the limitations of conventional homogeneous degradable materials and enables precise drug delivery in synergy with other functional agents (such as antioxidants and antimicrobial components), creating a healing-promoting microenvironment during degradation [15,27].

Therefore, based on the stabilizing effect of RHP on enzyme activity, this study developed self-biodegradable PCL/PU composite suture using electrospinning technology. By designing an enzyme loading gradient, precise control over the degradation period was achieved, effectively matching the healing time windows of different tissues. Furthermore, the suture incorporates functional active agents, enabling synergistic antioxidant and antibacterial effects during the self-biodegradation.

2. Materials and Methods

2.1. Chemical synthesis of PU and RHP

The PU synthesis was performed according to the reported method with some modified under stoichiometric conditions (NCO/OH = 1) [28,29]. PCL and methylene diphenyl diisocyanate (MDI) were separately dissolved in dimethyl sulfoxide (DMSO), then introduced into the reactor, and the polymerization reaction was initiated under mechanical stirring (500 $r \cdot min^{-1}$) at 80 °C for 6 h.

The preparation method of RHP was based on the previous methods in our laboratory [16]. RHP was synthesized by mixing methyl methacrylate, ethylene glycol methyl ether methacrylate, 2-ethylhexyl methacrylate and potassium 3-(methacryloyloxy) at a ratio of 2:4:2.5:0.5 (mol). The number–average molecular weight molecular weight of RHP was 19.30 kDa.

2.2. The protective ability of RHP to BCL in organic reagents

BCL was desalted using an AKTA protein purifier and the enzyme concentration was determined using a BCA protein assay kit. RHP was added to the BCL aqueous solution at a molar ratio of 100:1 (RHP/BCL), followed by incubation at 30 °C with agitation at 200 $r \cdot min^{-1}$ for 10 min.

The diameter of BCL-RHP was characterized by dynamic light scattering (DLS, Zetasizer Nano ZS90). The CLSM was performed on a Leica TCS SP5 confocal microscope. Sulforhodamine 101, and BCL-GFP were excited using a HeNe 580 nm laser and a 488 nm argon ion laser. Emission was detected between 580 and 650 nm for Sulforhodamine 101, and between 495 and 545 nm for BCL–GFP.

The mixture was freeze-dried to obtain the BCL-RHP complexes. The residual enzyme activity of BCL and BCL-RHP complexes were measured by the reaction with (4-nitrophenyl)octanoate (*p*-NPO) after 4 h exposure in different organic solvents including (2,2,2-trifluoroethano (TFE), ethanol

(EtOH), dichloromethane (DCM), DMSO), phosphate–buffered Saline (PBS buffer) was used as control. The generation of *p*-nitrophenol was recorded at the wavelength of 410 nm.

2.3. Preparation of self–biodegradable PCL/PU composite suture

The preparation of PCL/PU composite suture was fabricated using an electro–microfluidic spinning device (Nanjing Janus New–Materials Co. Ltd). PCL and PU were dissolved in TFE at room temperature for 12 h to dissolve completely with a certain mass ratio (100/0, 90/10, 80/20, 70/30, 60/40, 50/50) with a total polymer concentration of 130 $mg \cdot ml^{-1}$. Based on the optimal PCL/PU ratio, BCL–RHP complexes were incorporated at concentrations of 0.05%, 0.1%, and 0.5% (mass), respectively. According to the previous report [16], the solution was loaded into an injection pump at a rate of 0.5 $ml \cdot h^{-1}$, making the nozzle (20G) connect to the voltage supply at 18 kV. The receiver keeping a speed of 200 $r \cdot min^{-1}$ and distance of 10 cm away from the nozzle. After spinning for 2 h, the collected sutures were removed and dried in vacuum to remove residual solvent.

2.4. Mechanical test

The tensile strength and elastic modulus of composite sutures were performed in accordance with an electro-mechanical universal tensile testing machine (Ts9105-R, SANS, USA). Two ends of the suture with a total length of 15 cm were fixed to a clamp with a spacing of 5 cm, and elongated at a 10 $mm \cdot min^{-1}$ rate with a load of 500 N at room temperature. Stress–strain curves were recorded when the suture was broken. Three independent replicate experiments were conducted for each sample.

2.5. Degradation of the self-biodegradable PCL/PU composite sutures

The sutures (10 cm per piece) were fully immersed in PBS buffer (pH 7.4), simulated body fluid (SBF) and simulated wound fluid (SWF) at 37 °C for 15 days to observe the degradation. Each sample formulation was prepared and tested in triplicate. SBF was purchased from Beijing Leagene Biotechnology Co., Ltd. The formulation of SWF was modified based on reported method with some modified [30]: 29 $g \cdot L^{-1}$ bovine serum albumin (BSA), 18.8 $mmol \cdot L^{-1}$ ethyl lactate, 105 $mmol \cdot L^{-1}$ creatinine, 2.5 $mmol \cdot L^{-1}$ $CaCl_2$, 2.7 $mmol \cdot L^{-1}$ KCL, 0.5 $mmol \cdot L^{-1}$ $MgCl_2$, 142 $mmol \cdot L^{-1}$ NaCl, 0.7 $mmol \cdot L^{-1}$ glucose, and 9.6 $mmol \cdot L^{-1}$ urea.

During the degradation process, the suture samples were photographed every 5 days. The residual sutures were analyzed using scanning electron microscopy (SEM, Hitachi Regulus 8100) and gel permeation chromatography (GPC, Waters 1515) at the end. The degradation metabolites were subsequently analyzed by high-performance liquid chromatography (HPLC, Agilent 1200 series) equipped with a reverse-phase C18 HPLC column and a DAD-detector. The elution and detection protocol were according to the reported methods [31]. Mass spectrometry (MS) analysis using an Agilent 6530 Q-TOF instrument in negative ion mode with electrospray ionization (ESI). Instrument parameters were set as follows: capillary voltage at 3.5 kV, gas temperature at 350 °C, drying gas flow rate of 5 $L \cdot min^{-1}$, Oct 1 RF Vpp at 750 V, and m/z range of 50–750.

2.6. Cytocompatibility assessment

The degradation products of PCL/PU-0.5%BCL and PCL/PU–0.5%BCL/RHP were lyophilized and then sterilized by ultraviolet irradiation. The biocompatibility evaluation comprised four experimental groups: (1) negative control (cell culture medium), (2) degraded PCL/PU–0.5%BCL, (3) degraded PCL/PU-0.5%BCL/RHP, and (4) positive control (20% DMSO). Each treatment was performed in triplicate wells within a single experiment, and the entire experiment was independently repeated three times. Suture segments (2.00 ± 0.05 cm) underwent sequential sterilization: immersion in 750 $ml \cdot L^{-1}$ ethanol (15 min, 25 °C) followed by triple PBS rinsing. L929 cells in logarithmic growth phase were seeded into 48–well plates at 1×10^4 cells per well, and maintained under standard culture conditions (37 °C, 5% CO_2, 95% humidity). At 1, 3, and 7 days, culture medium was carefully removed and each well was washed three times with PBS. 500 ml serum-free medium containing 10% CCK-8 reagent was added to each well and incubated at 37 °C for 2 h, and the absorbance at 450 nm was measured using a microplate reader to detect cellular metabolic activity.

2.7. Functional characterization of thymol–loaded self–biodegradable sutures

Thymol was loaded onto the sutures by dissolving and mixing it into the polymer solution with 1.5% (mass) prior to electrospinning. Each functional suture sample (PCL/PU-0.5%BCL@Th and PCL/PU-0.5%BCL/RHP@Th) was tested in triplicate (10 cm per piece). The controlled degradation studies were conducted in PBS (pH 7.4, 37 °C) at a theoretical thymol concentration of 0.5 $mg \cdot ml^{-1}$ (calculated based on 100% release efficiency). During the degradation process, the release amount of thymol in the system and the ABTS free radical scavenging activity were measured at 0, 4, 8, 12, 24, 36, 48, and 72 h, respectively. The concentration of thymol in the degradation medium was quantified *via* HPLC with a calibration curve according to the reported method [32]. ABTS radical scavenging rate = $[1-(A_1-A_2)/A_0] \times 100\%$. A_0: Initial absorbance control group, absorbance value of the mixture containing only the ABTS radical working solution, (without the sample to be tested). Absorbance value of H_2O at 734 nm. A_1: Absorbance of the sample test group, absorbance value of the mixed system containing the test sample and ABTS radical working solution after the reaction has ended. Absorbance value at 734 nm of the reacted sample. A_2: Blank control absorbance, absorbance value of the mixed system containing the test sample but no ABTS radicals (used to subtract interference from the sample solution's own color or turbidity on absorbance readings). Absorbance values measured at 734 nm after reaction with PBS instead of the sample to be tested. Post–degradation antimicrobial activity was evaluated against gram–negative (*Escherichia coli* ATCC 25922) and gram-positive (*Staphylococcus aureus* ATCC 29213) strains. Overnight cultures in LB broth were standardized to 10^7 $CFU \cdot ml^{-1}$ using sterile saline. 50uL bacterial cultures was added in 4 ml degraded medium. All groups were incubated at 200 $r \cdot min^{-1}$ at 37 °C for 12 h. The absorbance at 600 nm was obtained on hours 6 and 12 to examine the growth of bacteria.

2.8. Statistical analysis

Quantitative data were shown as mean ± standard deviation (SD). The significance between groups was assessed by unpaired Student's *t*-test or one-way analysis of variance. The differences were considered significant at $p < 0.05$. The graphs and statistical analysis were carried out using SPSS software, version 7, and OriginPro 2020 (Learning Edition). For data with standard deviation, it is common practice to conduct at least three independent experiments to ensure the reliability of the results.

3. Results

3.1. The encapsulation and protective effects of RHP on BCL

After interacting with RHP, the complex had a diameter of (222.7 ± 9.4) nm (PDI 0.445) with a narrow size distribution (Fig. 1(a)), and the BCL underwent a transition formed a state of large–area aggregation to a monodispersed state and was encapsulated by the RHP (Fig. 1(b)). The relative enzyme activity of BCL and BCL-RHP in different organic reagents was analyzed to verify the protective effect of RHP on BCL. The enzyme activity of BCL significantly declined in various organic reagents, particularly in trifluoroethanol, where the enzyme activity retention rate was less than 10%. However, under the protection of RHP, the relative enzyme activity retention rate remained above 60% (Fig. 1(c)). This protective effect was further verified following the electrospinning process. The PCL/PU group and the PCL/PU-0.5% BCL group showed no degradation due to the loss of enzyme activity, while the PCL/PU-0.5% BCL/RHP composite suture exhibited degradation-triggered activity characteristics: no enzyme activity was detected during the initial stage, as the absence of suture degradation prevented substrate-enzyme contact. However, after 15 days of degradation, with the depolymerization of PCL/PU, BCL became exposed, and residual enzyme activity was detected at a relatively high level (Fig. S1).

3.2. Optimization of PCL/PU composite ratio and characterization of self–biodegradable sutures

The mechanical properties of PCL/PU composite sutures varied significantly with composition (Fig. 2(a)). As the PU content increased from 10% to 50%, the sutures strain first increased from 401.57% ± 12.84% to 449.01% ± 24.97%, then sharply decreased to 64.86% ± 7.37%, demonstrating PU's effective role in modulating ductility. Correspondingly, the tensile strength showed steady enhancement from (12.13 ± 0.82) MPa to (28.44 ± 1.25) MPa within the 10%–30% PU range, but decreased to (12.52 ± 1.53) MPa and (10.06 ± 0.97) MPa at 40% and 50% PU, respectively. Young's modulus, calculated from the initial linear region of the stress–strain curves, initially increased then decreased with the content of PU increases, peaking significantly at (42.43 ± 5.3) MPa ($p < 0.05$) for the PCL70/PU30 group (Fig. 2(b)). Based on optimal strength–ductility balance, 30% PU content was selected for subsequent studies.

BCL was gradient-loaded (0.05%–0.5% (mass)) into PCL70/PU30 sutures using the RHP encapsulation system. Mechanical testing revealed that enzyme loading increased elongation at break (343.12% ± 14.12% to 467.37% ± 10.95%), decreased tensile strength ((28.78 ± 1.57) MPa to (23.82 ± 2.34) MPa), reduced Young's modulus (Fig. 2(c) and (d). Both PCL/PU–0.1%BCL/RHP and PCL/PU-0.5%BCL/RHP showed significant differences from PCL/PU–0.5%BCL. The plasticizing effect [33] of the BCL-RHP complex within the fiber matrix stems from its hydrophilic and polar groups, which engage in molecular-level interactions with the polymer matrix. These interactions partially disrupt the original interchain stacking and hydrogen bond formation, rendering the fiber more susceptible to elastic deformation at the macroscopic level. This manifests as increased flexibility and reduced modulus. Fig. 3(a) and (b) show the macroscopic appearance and microscopic morphology, respectively, of the self-biodegradable PCL/PU composite sutures. The BCL/RHP-loaded sutures consisted of "bead-on-string" nanofibers. As the BCL loading increased, the hydrophilicity of the sutures progressively enhances, with the water contact angle decreasing from 115.31°± 2.51° to 0.35°± 0.02° (Fig. 3(c)).

3.3. Analysis of degradation performance of self-biodegradable sutures

The regulatory effects of enzyme loading on suture degradation were assessed in three physiological solutions: phosphate-buffered saline (PBS, pH 7.4), simulated body fluid (SBF), and simulated wound fluid (SWF) (Fig. 4). In the PBS environment, the 0.05% (mass), 0.1% (mass), and 0.5% (mass) groups exhibited softening in 15, 10 and 5 days, respectively. The 0.5% (mass) group showed fragmentation, transparency, and solution turbidity by day 15, indicating substantial oligomer dissolution. In contrast, only suture breakage was observed in the SBF environment, without significant softening or transparency changes. The sutures exhibited the highest degradation activity in the SWF environment: the 0.05% (mass) group caused solution turbidity at 15 days, the 0.1% (mass) group reached a semi-dissolved state, and the 0.5% (mass) group exhibited complete fiber disintegration with no intact suture structure remaining. In the control group, which contained no added enzymes or enzyme complexes, no degradation occurred after 15 days of incubation in all three *in vitro* environments (Fig. S2).

The degradation process of self-biodegradable sutures was further analyzed by SEM and GPC. After 15 days in PBS, SEM revealed progressive softening of the nanofiber with the increasing enzyme content. The structure of nanofibers in the 0.5% (mass) group had completely disappeared, forming a colloidal matrix (Fig. 5(a)–(d)). The molecular weight distribution curves of the degradation residues showed a leftward shift relative to the

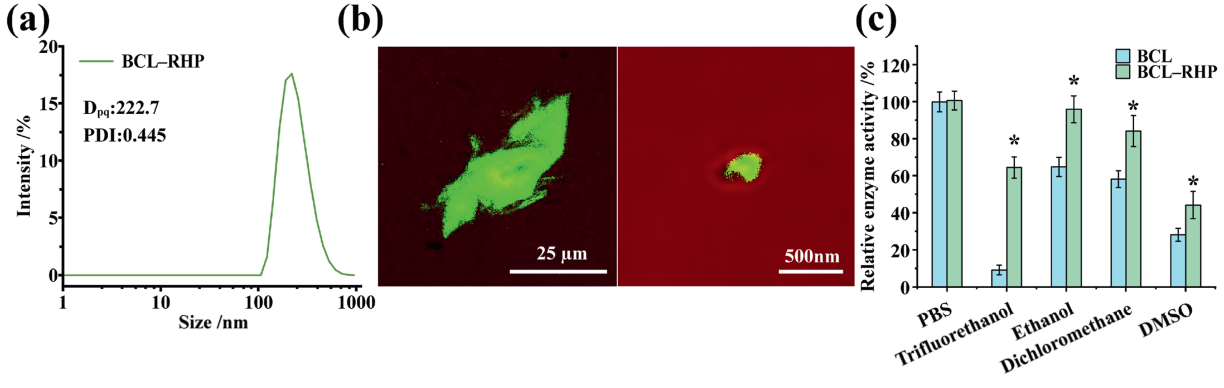


Fig. 1. (a) DLS results of BCL–RHP in water. (b) CLSM images of BCL (the left) and RHP–BCL (the right). (c) Relative enzyme activity of BCL and RHP–BCL in different organic solutions.

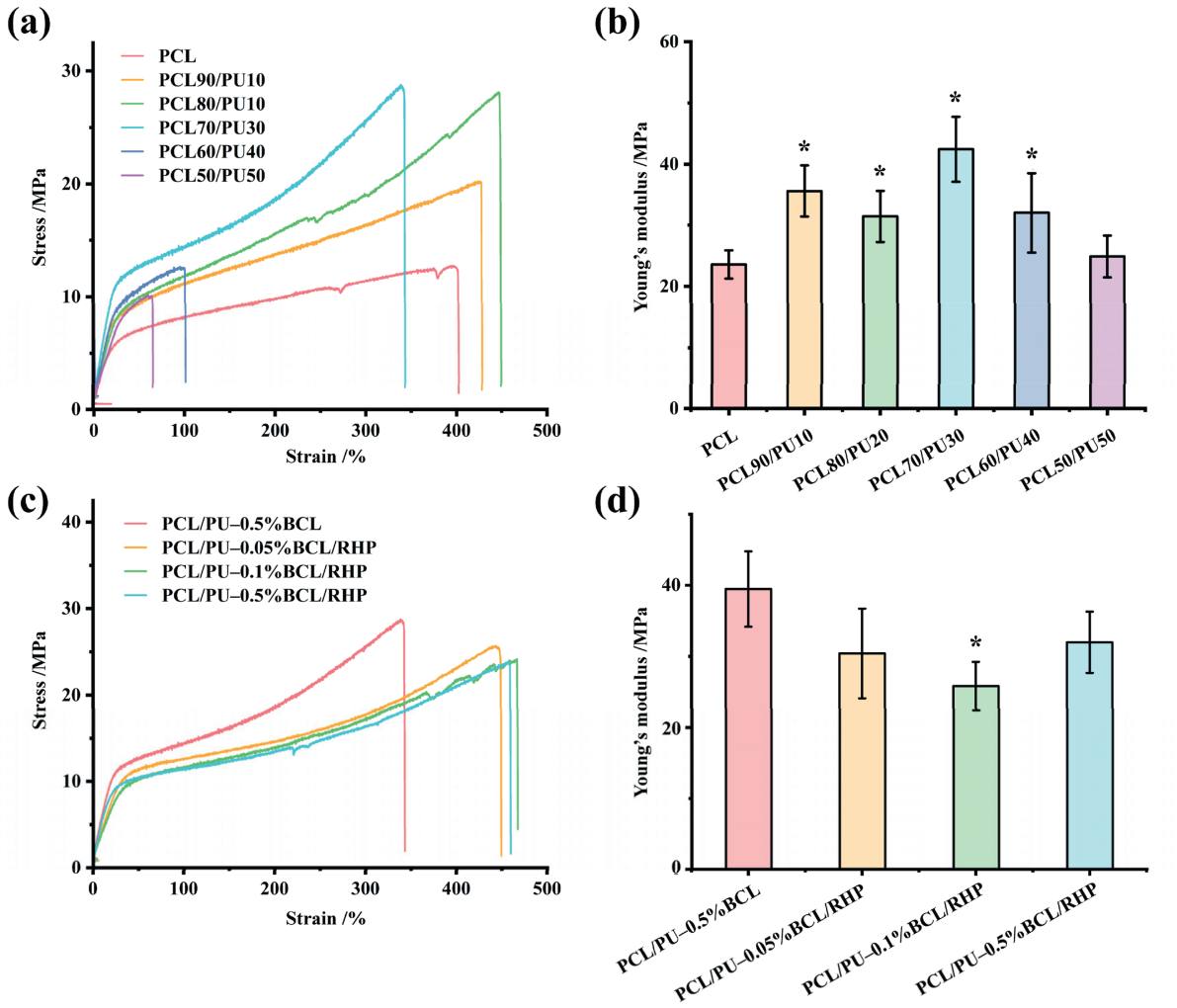


Fig. 2. Mechanical properties of PCL/PU composite sutures. (a) Stress–strain curve of composite sutures with different PCL/PU ratio, and statical ANOVA analysis for (b) Young's modulus. (c) Stress–strain curve of PCL/PU composite sutures with different enzyme contents, and statical ANOVA analysis for (d) Young's modulus.

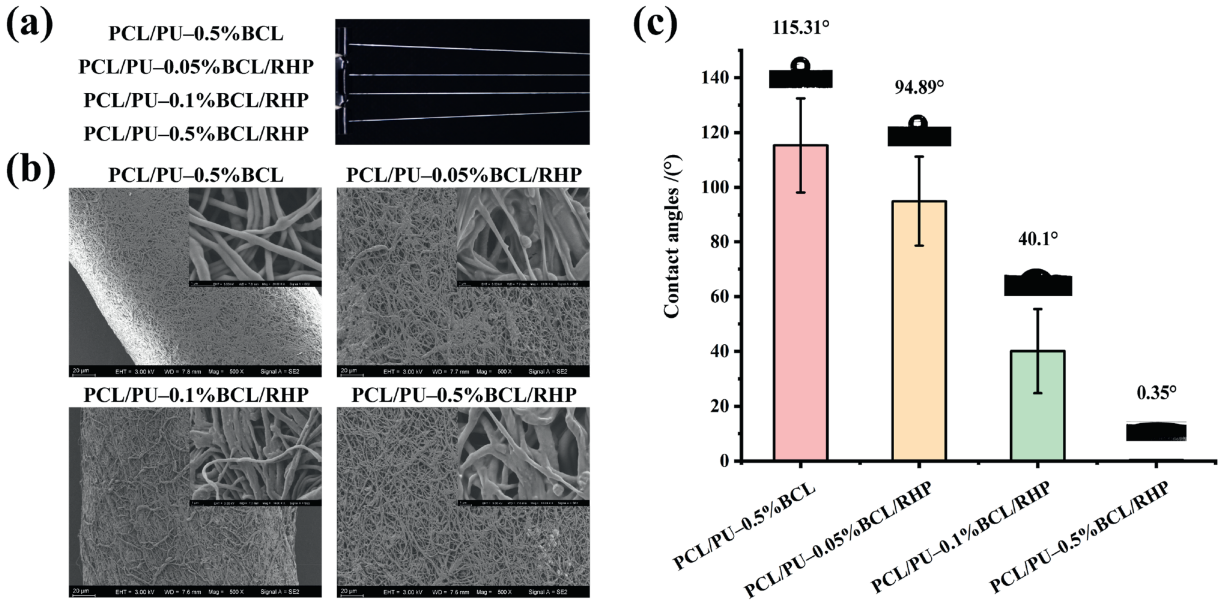


Fig. 3. (a) Representative images of composite sutures in each group. (b) SEM images of PCL/PU-0.5%BCL, PCL/PU-0.05%BCL/RHP, PCL/PU-0.1%BCL/RHP and PCL/PU–0.5%BCL/RHP monofilament at different magnifications of 500× and 10000×. (c) Contact angle of water on self-biodegradable PCL/PU composite sutures with different enzyme contents.

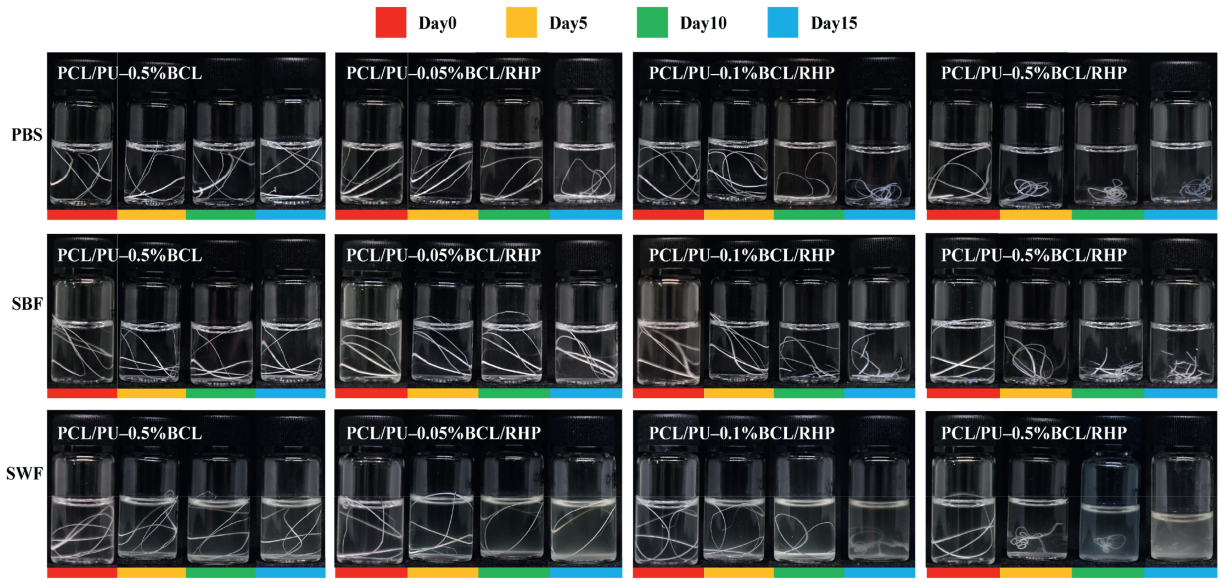


Fig. 4. Representative images of self-biodegradable PCL/PU composite sutures with different enzyme contents after 15 days of immersion in PBS, SBF and SWF.

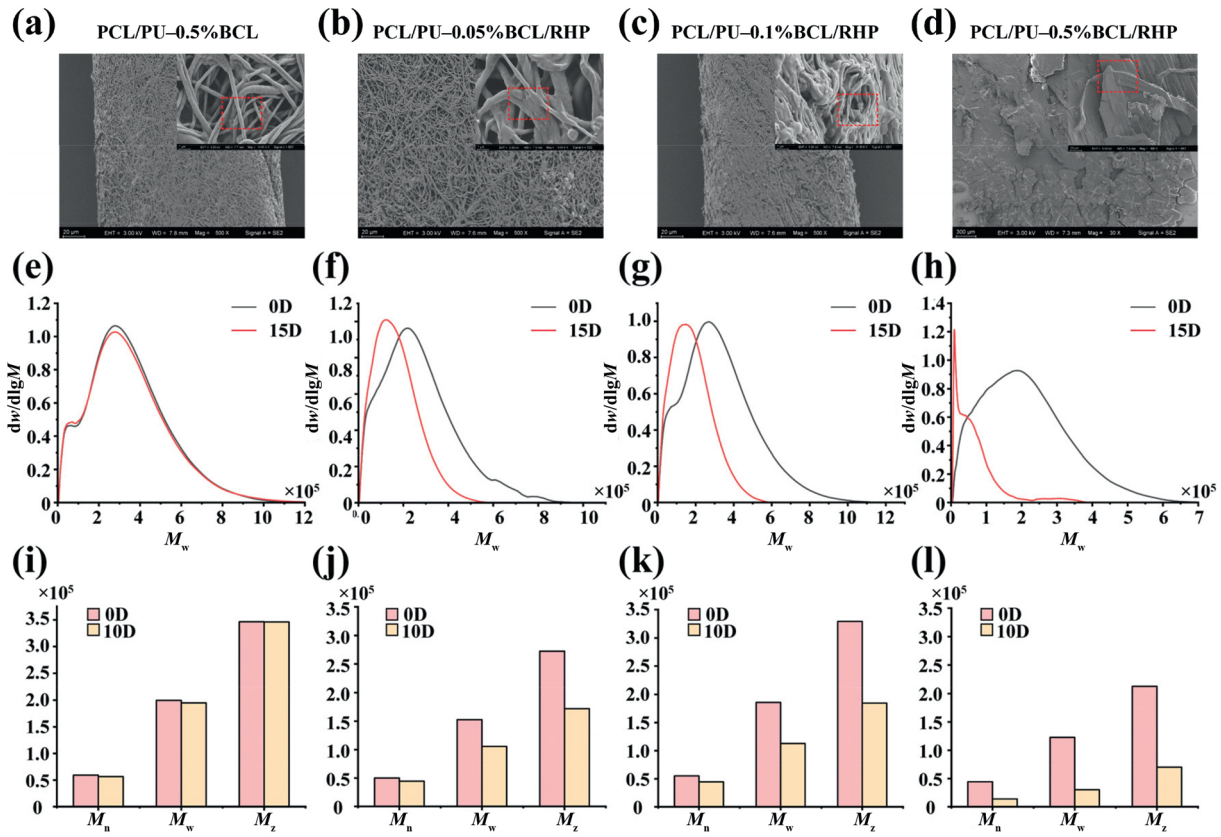


Fig. 5. (a–d) SEM images, (e–h) molecular weight distribution plots and (i–l) M_n, M_w and M_z of self–biodegradable PCL/PU composite sutures with different enzyme contents after 15 days of immersion in PBS. The dashed box indicates the progressive deformation and eventual disintegration of the nanofibers as a result of enzymatic degradation.

undegraded control (Fig. 5(e)–(h)). Specifically, the Z-average, weight-average, and number–average molecular weights decreased. For the 0.05% (mass), 0.1% (mass), and 0.5% (mass) groups, the reductions were 11.18%, 19.57%, and 69.89% for M_z 30.79%, 39.33%, and 75.62% for M_w; and 36.88%, 43.95%, and 66.82% for M_n, respectively (Fig. 5(i)–(l)). In contrast, the blank control group showed no degradation over the same period, with its M_n, M_w, and M_z, remaining essentially unchanged (only minor fluctuations within measurement error), confirming the material's inherent resistance to hydrolysis (Fig. S3). This study systematically evaluated the degradation behavior of suture materials with different compositions under enzymatic action and its impact on mechanical properties through *in vitro* degradation experiments. The experimental setup included a blank control group (PCL/PU),

an uncoated BCL group (PCL/PU-0.5%BCL), and three experimental groups with varying enzyme concentrations (PCL/PU-0.05%BCL/RHP, PCL/PU-0.1%BCL/RHP, PCL/PU-0.5%BCL/RHP), each comprising three parallel samples. Degradation experiments involved sampling at 3-day intervals to continuously monitor mass loss and changes in mechanical properties. Due to the faster degradation rate of samples with 0.5% enzyme content, the initial test interval was set to 1 day. Results showed that neither the blank group nor the unencapsulated BCL group exhibited significant degradation during the experimental period, with negligible mass loss. In contrast, the enzyme-containing experimental groups exhibited significantly increased degradation rates with rising enzyme concentrations. By 15 days, the mass loss rates for the 0.05%, 0.1%, and 0.5% BCL/RHP concentration groups reached 18.47%, 31.59%, and 92.18%, respectively (Fig. S4). Analysis of molecular weight changes indicated a gradual shift of the main peak toward the lower molecular weight region as degradation progressed, suggesting polymer chain scission. This trend is consistent with a bulk degradation mechanism, where enzymes penetrate the material interior to cleave chains, rather than being confined to surface erosion. Mechanical testing revealed a concomitant decline in tensile strength and other key properties (*e.g.*, elastic modulus, elongation at break). Notably, in the 0.5% enzyme group, these properties had diminished to minimal levels by day 9 (Fig. S5). Mechanical property tests conducted on samples degraded over different time periods revealed that the mechanical properties of the PCL/PU and PCL/PU–0.5%BCL groups showed no significant decline after 15 days. In contrast, the PCL/PU–0.05%BCL/RHP, PCL/PU-0.1%BCL/RHP, and PCL/PU-0.5%BCL/RHP exhibited distinct differences in mechanical properties as degradation progressed. Samples with 0.05% BCL showed a significant decrease in tensile strength by day 9. During the initial stage of wound healing, sutures must maintain sufficient tensile strength to close the wound and withstand tissue forces. As healing progresses, they should degrade controllably, gradually transferring load to the forming tissue to avoid complications like foreign body reactions or mechanical mismatch caused by prolonged retention. In this study, the high-enzyme-concentration group experienced an earlier decline in mechanical properties. This indicates that, in practice, the suture's degradation profile need to be precisely tuned to match the anticipated healing timeline of the target tissue, thereby achieving an optimal balance between temporary mechanical support and timely absorption. The prepared biodegradable sutures were stored at 4 °C for one year to simulate long–term inventory conditions in actual medical settings. Subsequent degradation testing revealed significant morphological changes in the PCL/PU–0.5%BCL/RHP sutures after a 15-day degradation process (Fig. S6). The results indicate that even after one year of storage, the suture's degradation capability remained fully intact. This not only directly demonstrates that the loaded enzymes retain excellent biological activity after prolonged storage but also confirms that the entire BCL/RHP system possesses outstanding storage stability. This stability sufficiently meets the dual requirements for suture shelf life and performance stability in actual clinical applications. The result of HPLC proved the increased production of 6-hydroxycaproic acid, the monomer of PCL, with increasing the content of enzyme (Fig. 6(a)). MS data revealed that monomers ($m/z = 131.07$) and dimers ($m/z = 245.14$) were present after the degradation of 0.5% (mass) suture in PBS for 15days (Fig. 6(b)–(c)).

3.4. In vitro cell viability

Biological evaluation of sutures is critical for analyzing whether they induce any type of toxicity at the cellular level. The effects of 20% DMSO and the degradation products of PCL/PU-0.5%BCL and PCL/PU–0.5%BCL/RHP sutures on cell viability were assessed using the L929 mouse fibroblast cell line at 1, 3, and 7 days. Representative images of each group in Fig. 7(a)–(b) show there were no significant changes in cell morphology and viability after co-incubation with the degradation products of self-biodegradable PCL/PU sutures for 7 days compared to the control group, while nearly all cells in the 20% DMSO group died. These results indicate low acute toxicity and good biocompatibility of self-biodegradable sutures.

3.5. Functionalized self–biodegradable sutures

The thymol release curve of self-biodegradable PCL/PU sutures was shown in Fig. 8(a). Thymol was rapidly released within the first 12 h, reaching 35.35% ± 1.95%, followed by sustained release reaching a cumulative amount of 86.76% ± 1.34% at 120 h. This represented a 5–fold increase over non-degradable PCL/PU sutures (18.01% ± 1.07%). The ABTS radical scavenging rate increased from an initial 3.71% ± 0.31% to 79.85% ± 3.65% at 120 h during degradation (Fig. 8(b)), demonstrating that the degradable PCL/PU sutures exhibit sustained antioxidant capacity with the release of thymol.

In the end of degradation, the degradation solution was mixed with LB medium and inoculated with *Staphylococcus aureus* and *Escherichia coli*. As shown in Fig. 8(c)–(f), both the PCL/PU-0.5%BCL/RHP@Th group and the 0.5 $mg \cdot ml^{-1}$ thymol group exhibited significant inhibition of *S. aureus* (OD_{600} reduction by 82.99% and 83.41%, respectively), whereas neither inhibited *E. coli*. The 1 $mg \cdot ml^{-1}$ thymol group completely inhibited both strains ($OD_{600} < 0.3$).

4. Discussion

As amphiphilic compounds, surfactants have demonstrated effectiveness in preserving enzymatic stability within self-degrading materials. For instance, the encapsulation of lipase by Tween 20 [22] or the triblock copolymer Pluronic F-127 [34] can maintain the structural stability of enzymes during high-temperature processing and in organic solvent environments, though degradation efficiency remains limited. Designed based on protein sequence trends and surface chemical characteristics, RHP provide a protective barrier for enzymes against organic solvent exposure and conformational changes by mimicking the dynamic binding mechanism of natural chaperone proteins [25]. Notably, RHP not only exhibit amphiphilicity but also possess intrinsic protein-stabilizing capabilities. The protective capability of RHP enables efficient degradation of PCL film within 24 h at a BCL loading of 0.02% (mass) [23]. Additionally, encapsulating BCL with RHP can control the particle size of the enzymes complex at the nanoscale, enhancing dispersion in organic reagents and enabling chain-end-mediated depolymerization of polyesters [23], thereby achieving complete depolymerization while reducing the generation of microplastics.

As one of the most prevalent clinical implants, sutures fundamentally maintain tissue apposition until wounds regain tensile strength to withstand physiological stress. Surgical sutures require robust mechanical properties for effective wound closure, with tensile stress testing serving as a fundamental metric for assessing fracture resistance. The results showed that PCL70/PU30 suture exhibited the optimal tensile strength, stress, and Young's modulus among all tested groups, without significant reduction in elongation at break, which is attributable to PU's inherently higher stress values compared to PCL [35]. Incorporating PU at appropriate ratios

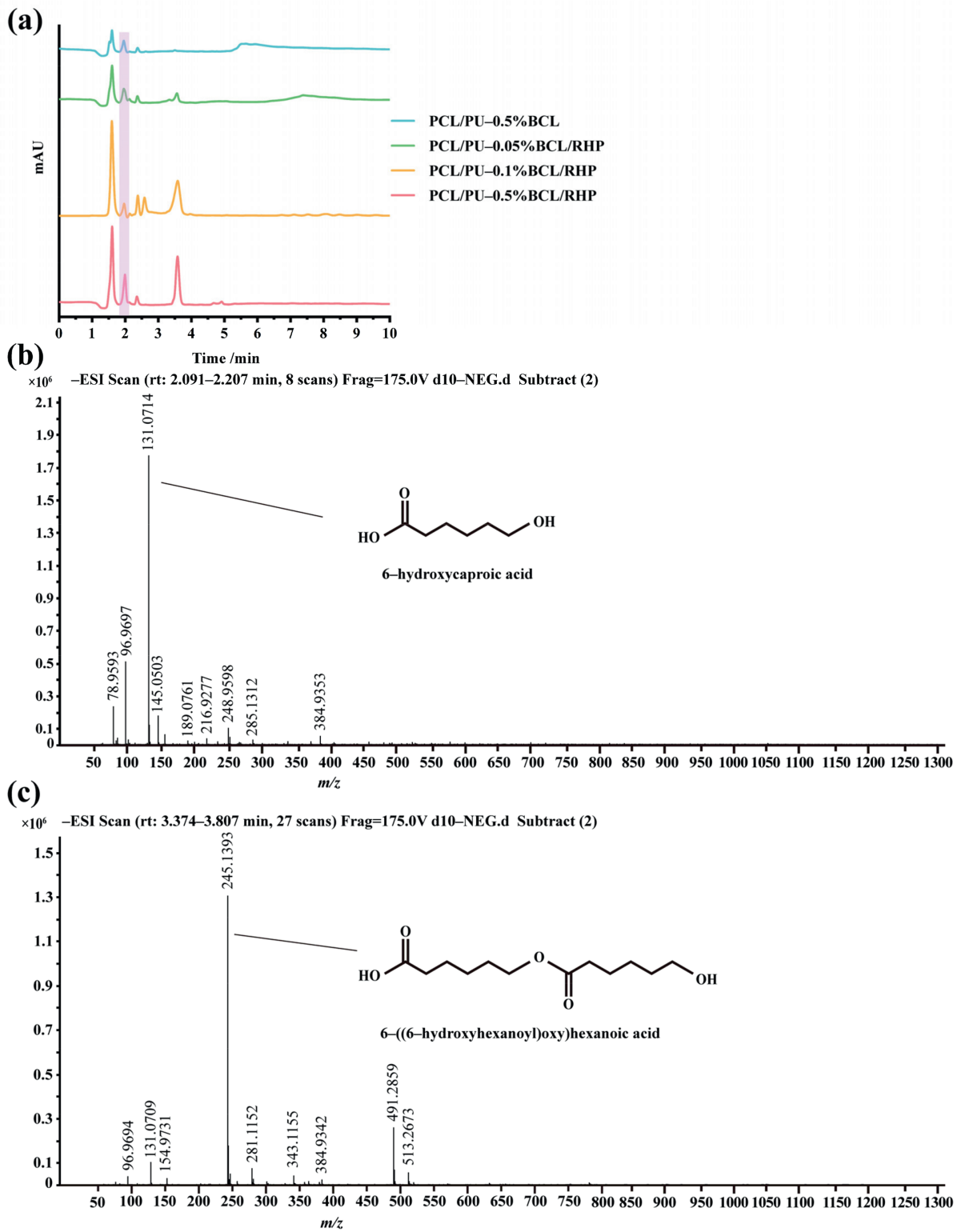


Fig. 6. (a) HPLC analysis of degradation products of self–biodegradable PCL/PU composite sutures with different enzyme contents after 15 days of immersion in PBS. (b–c) The mass spectrum of 6-hydroxycaproic acid and 6-((6-hydroxyhexanoyl)oxy)hexanoic acid.

maintains tensile strength while enhancing Young's modulus of PCL, fulfilling the mechanical requirements of sutures.

After loading the BCL–RHP complex, the elongation at break of self–biodegradable sutures increased while Young's modulus decreased, indicating enhanced material plasticity and impact resistance. This stems from elevated exposure density of hydrophilic polyethylene glycol segments in RHP molecules, which simultaneously enhances hydrophilicity and strain rate. For example, hydrogel materials contained abundant internal water, exhibited strong plasticity, and showed good fluid thermodynamic properties

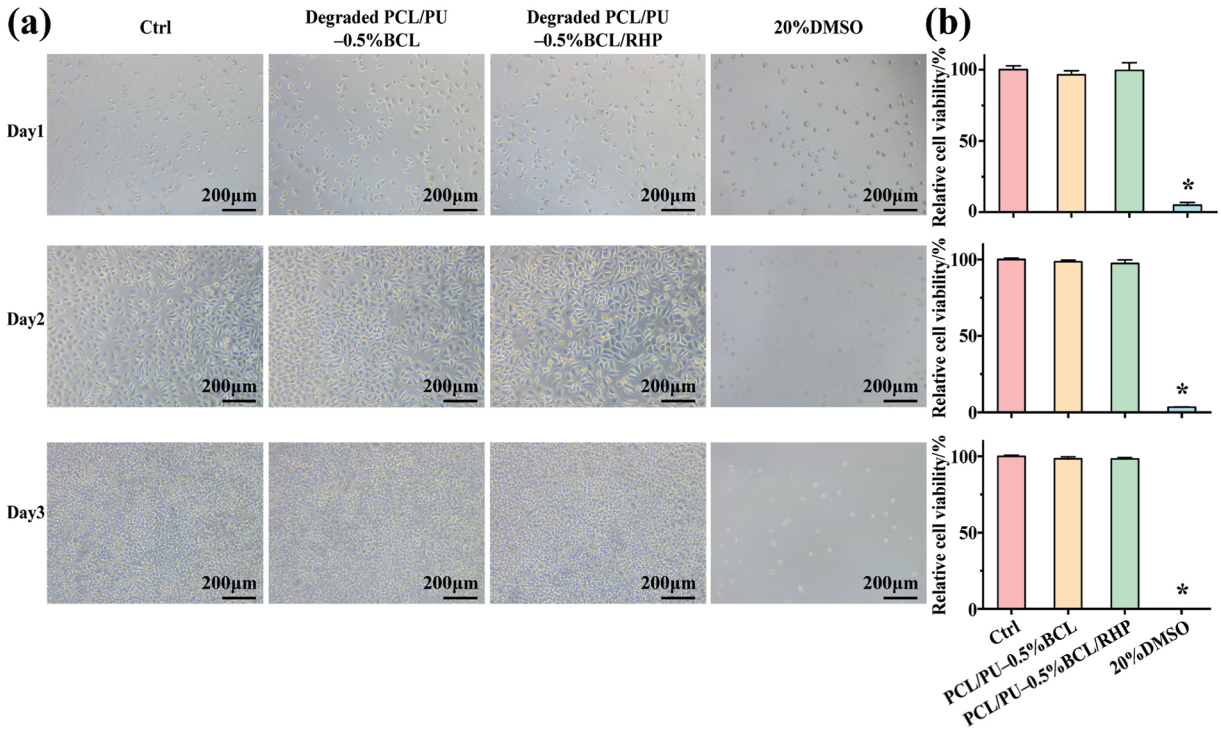


Fig. 7. (a) Representative images and (b) the viability changes of L929 cells co-cultured with degraded PCL/PU-0.5%BCL, degraded PCL/PU-0.5%BCL/RHP and DMSO for 1 day, 3 days, and 7 days.

and biocompatibility, but the strength and toughness of them were generally less than expected [36]. While enzyme-loaded sutures maintained visual homogeneity, their bead-on-string heterogeneous microstructure indicated successful enzyme incorporation. This structure increases the moisture sensitivity of nanofibers, enabling solution-mediated swelling to initiate spontaneous degradation through microreactor-like depolymerization [16]. Meanwhile, sufficient hydrophilicity provides the necessary conditions for self-biodegradable sutures to interact with cells and surrounding tissues in aqueous environments [37]. This controllable wettability regulation characteristic can provide an ideal interfacial condition for drug loading and cell adhesion.

The degradation rate of self-biodegradable sutures exhibited enzyme-concentration dependence across all solutions in this research. At an enzyme loading of 0.5% (mass), PCL/PU sutures degraded to a transparent state in PBS, showed fragmented morphology in SBF, and nearly complete degradation in SWF by day 15 respectively. This enhanced degradation in SWF likely stems from bovine serum albumin facilitation [38], while diverse ion composition in SBF leads to degradation patterns distinct from those in PBS. The results of SEM revealed that fiber morphology gradually softened and disappeared with increasing enzyme concentration, confirming the controlled degradation process of the sutures. GPC analysis provided definitive evidence of plastic degradation, with left-shifted molecular weight distribution profiles and significant molecular weight reduction further validating the process. *In vitro* experiments show that sutures with a 0.5% (mass) enzyme load degrade completely within about 15 days under simulated conditions, a timeframe that aligns closely with the critical two-week phase of conventional wound healing. This *in vitro* temporal alignment suggests the material may facilitate synchronized degradation and repair *in vivo*. Such synchronization could minimize scar formation and secondary injury caused by a mismatch between healing and degradation timelines [16], Verification of this synchronous efficacy will be a key objective of subsequent *in vivo* studies. 6-hydroxyhexanoic acid (6-HA) and its dimer were detected in degradation products. As a medium-chain fatty acid, 6-HA has been shown to reduce inflammatory marker levels in high-fat diet-induced obese mice and 3T3-L1 cells [39], demonstrating wound-healing promotion potential and highlighting the advantages of PCL as a self-biodegradable suture material. In accordance with ISO 10993-5 standards, the degradation products from sutures loaded with 0.5% (mass) enzyme showed no significant adverse effects on the relative growth rate or morphology of fibroblast cells, which confirms the biocompatibility for medical device applications [40] and establishing foundations for future development.

Building upon self-biodegradation capability, sutures can be further functionalized through the incorporation of bioactive agents such as basic fibroblast growth factor, gentamicin, and anions [40,41] to accelerate granulation tissue formation and inhibit bacterial growth. This study engineered antioxidant and antibacterial functionality into self-degrading sutures through thymol incorporation——a polyphenolic compound critical for wound healing. The release of thymol exhibited characteristic biphasic kinetics: an initial burst within 12 h followed by sustained release over 120 h, enabling continuous delivery for over 5 days. This release behavior can be attributed to RHP significantly enhancing the material's hydrophilicity, as evidenced by contact angle measurements, which promotes rapid suture wetting and accelerates the initial dissolution of thymol, resulting in an initial rapid—release phase. The subsequent sustained slow release primarily stems from the nanofiber structure's inherent characteristics, including small pore size, low porosity, and tortuous diffusion pathways, as confirmed by morphological observation, which collectively retard molecular diffusion.

With the development of smart materials, sutures that can degrade or even be completely absorbed *in vivo* are crucial for preventing postoperative infections and alleviating patient discomfort. While current absorbable sutures rely on inherent

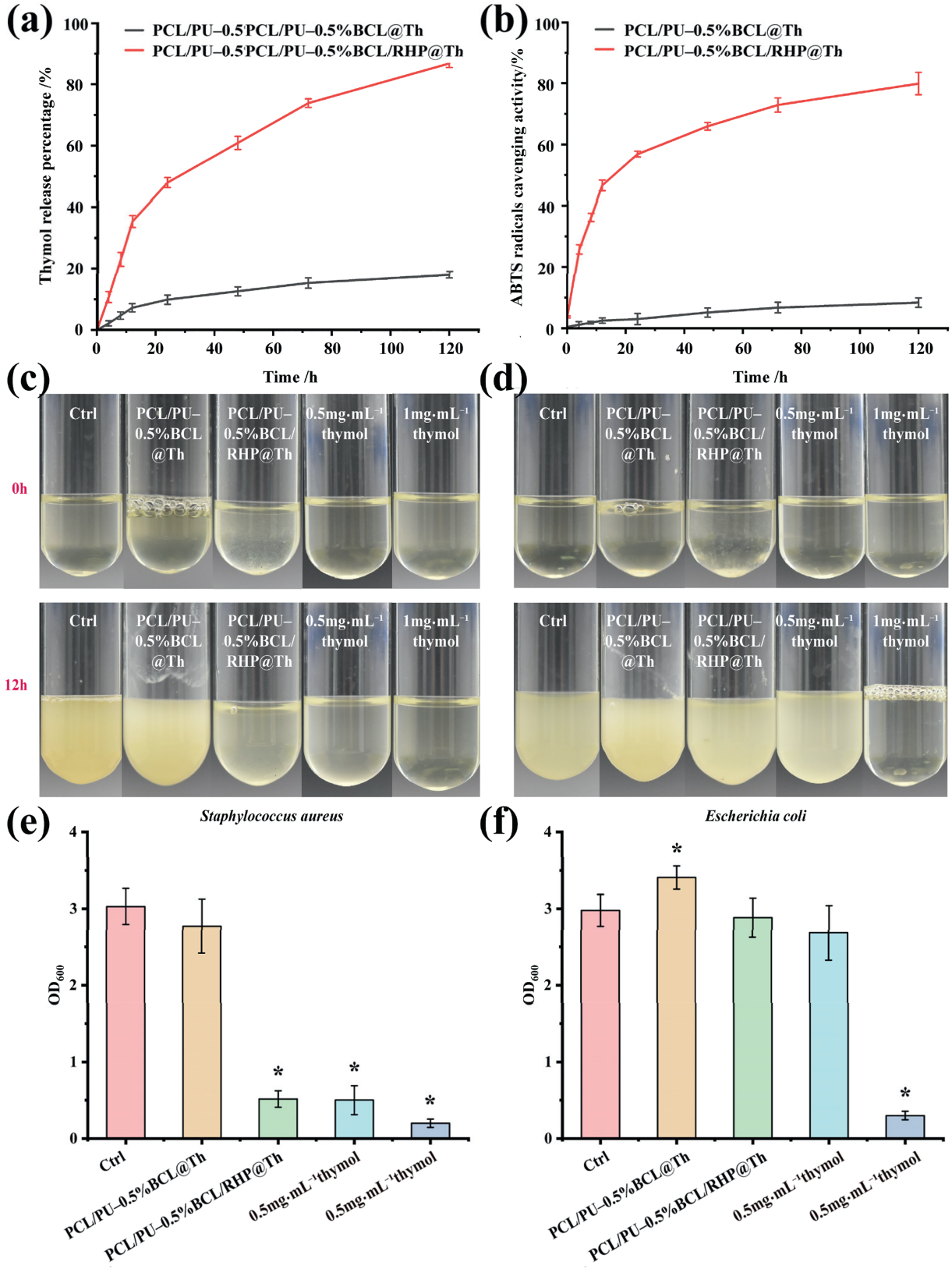


Fig. 8. (a) ABTS radical scavenging effects and (b) the release curves of thymol of PCL/PU-0.5%BCL@Th and PCL/PU-0.5%BCL/RHP@Th. (c–f) Images and OD_{600} value of thymol-loaded self-degrading composite sutures against *S. aureus* and *E. coli*.

material degradability, non-absorbable suture materials such as nylon, polypropylene (PP), polyester (PET) have often been overlooked due to their resistance to degradation. In recent years, with the continuous expansion of microbial/enzymatic libraries for non-degradable polymer materials, such as the achievement of 100% enzymatic depolymerization of PET [42], has provided more

options for enzyme-loaded materials. Thus, in addition to biodegradable polymers, non-degradable polymers may also achieve controllable degradation through the loading of specific enzymes.

5. Conclusions

This study successfully presents a self-biodegradable PCL/PU composite suture incorporating RHP–stabilized enzyme and functional agents to overcome the mismatch between the rate of wound repair and suture absorption in surgical wound management. RHP encapsulation can retain the degradation activity of BCL in organic solvents, enabling solvent-based electrospinning while preserving enzymatic functionality. Precise control over degradation timeline was achieved through enzyme–loading gradients, this controllable degradation enables the suture to match specific tissue healing time windows *in vivo*, although actual synchronization requires further validation in more complex physiological settings. The optimized PCL70/PU30 composition provided robust mechanical properties, while thymol functionalization conferred sustained antioxidant and antibacterial effects. Crucially, complete depolymerization into biocompatible monomers eliminated the risks of microplastics, and the degradation products exhibit excellent cytocompatibility. This technology bridges material innovation with clinical needs, offering programmable degradation, multifunctionality, and ecological sustainability for applications in dynamic tissue repair and chronic wound management.

CRediT Authorship Contribution Statement

Jianqi Lu: Writing – original draft, Visualization, Validation, Methodology, Investigation, Data curation, Conceptualization. Lingling Fan: Validation, Investigation, Formal analysis, Data curation. Yihu Wang: Validation, Investigation, Data curation. Xiaoli Zhou: Writing – review & editing, Supervision, Project administration, Methodology. Yujia Peng: Writing – original draft, Visualization, Validation, Methodology, Conceptualization. Weiliang Dong: Writing – review & editing, Supervision, Project administration, Methodology, Funding acquisition, Conceptualization. Min Jiang: Writing – review & editing, Supervision, Resources, Methodology, Conceptualization.

Declaration of Competing Interest

The authors declare that they have no known competing financial interests or personal relationships that could have appeared to influence the work reported in this paper.

Acknowledgements

This work was supported by various sources, including the National Key Research and Development Program of China (2024YFA0919100), Jiangsu Basic Research Center for Synthetic Biology (BK20233003), and the Jiangsu Synergetic Innovation Center for Advanced Bio-Manufacture (XTB2203), and Jiangsu Province Natural Science Foundation for Youths (BK20240540).

Supplementary Material

Supplementary data to this article can be found online at https://doi.org/10.1016/j.cjche.2026.02.006.

Data availability

Data will be made available on request.

References

[1] S. Feizi, M. Ali Javadi, F. Javadi, P. Malekifar, H. Esfandiari, Suture-related complications after deep anterior lamellar keratoplasty for keratoconus, *Graefes Arch. Clin. Exp. Ophthalmol.* 262 (4) (2024) 1195–1202.
[2] K. Merkel, K. Grzybowska, A. Strach, M. Gierek, The degradation of absorbable surgical threads in body fluids: insights from infrared spectroscopy studies, *Int. J. Mol. Sci.* 25 (20) (2024) 11333.
[3] J.R. Wang, J. He, M.S. Zhu, Y. Han, R.H. Yang, H.W. Liu, X.J. Xu, X.D. Chen, Cellular heterogeneity and plasticity of skin epithelial cells in wound healing and tumorigenesis, *Stem Cell Rev. Rep.* 18 (6) (2022) 1912–1925.
[4] J. Szabelski, R. Karpiński, Short-term hydrolytic degradation of mechanical properties of absorbable surgical sutures: a comparative study, *J. Funct. Biomater.* 15 (9) (2024) 273.
[5] A. Shedoeva, D. Leavesley, Z. Upton, C. Fan, Wound healing and the use of medicinal plants, *Evid. Based Complement. Alternat. Med.* 2019 (2019) 2684108.
[6] P. Chansoria, A. Chaudhari, E.L. Etter, E.E. Bonacquisti, M.K. Heavey, J.Y. Le, M.K. Maruthamuthu, C.C. Kussatz, J. Blackwell, N.E. Jasiewicz, R.S. Sellers, R. Maile, S. M. Wallet, T.M. Egan, J. Nguyen, Instantly adhesive and ultra-elastic patches for dynamic organ and wound repair, *Nat. Commun.* 15 (1) (2024) 4720.
[7] B.G. Ongarora, Recent technological advances in the management of chronic wounds: a literature review, *Health Sci. Rep.* 5 (3) (2022) e641.
[8] A.M. Lock, R. Gao, D. Naot, B. Coleman, J. Cornish, D.S. Musson, Induction of immune gene expression and inflammatory mediator release by commonly used surgical suture materials: an experimental *in vitro* study, *Patient Saf. Surg.* 11 (2017) 16.
[9] Y.R. Li, Q. Meng, S.J. Chen, P.X. Ling, M.A. Kuss, B. Duan, S.H. Wu, Advances, challenges, and prospects for surgical suture materials, *Acta Biomater.* 168 (2023) 78–112.
[10] Z.Q. Sun, Y.F. Jin, J.B. Luo, L.P. Li, Y. Ding, Y. Luo, Y. Qi, Y.G. Li, Q.H. Zhang, K.R. Li, H.B. Shi, S.K. Yin, H.Z. Wang, H. Wang, C.Y. Hou, A bioabsorbable mechano-electric fiber as electrical stimulation suture, *Nat. Commun.* 15 (1) (2024) 8462.
[11] H. Meng, G. Li, Shape-memory and self-reinforcing polymers as sutures. Shape Memory Polymers for Biomedical Applications, Elsevier, 2015, pp. 81–300.
[12] S.M. Hong, J.Y. Yoon, J.R. Cha, J. Ahn, N. Mandakhbayar, J.H. Park, J. Im, G.S. Jin, M.Y. Kim, J.C. Knowles, H.H. Lee, J.H. Lee, H.W. Kim, Hyperelastic, shape-memorable, and ultra-cell-adhesive degradable polycaprolactone-polyurethane copolymer for tissue regeneration, *Bioeng. Transl. Med.* 7 (3) (2022) e10332.
[13] J.H. Qiu, H. Zhao, S.F. Luan, L. Wang, H.C. Shi, Recent advances in functional polyurethane elastomers: from·structural design to biomedical applications, *Biomater. Sci.* 13 (10) (2025) 2526–2540.
[14] E. Polykandriotis, J. Daenicke, A. Bolat, J. Grüner, D.W. Schubert, R.E. Horch, Individualized wound closure-mechanical properties of suture materials, *J. Personalized Med.* 12 (7) (2022) 1041.
[15] Y.Q. Ding, X.C. Wang, J.G. Liu, H.Q. Shen, Z. Wang, M.B. Xie, Y. Chen, A.R. Barcenas, Z.Y. Zhao, G. Li, A reduced graphene oxide-coated conductive surgical silk suture targeting microresistance sensing changes for wound healing, *Sci. China Technol. Sci.* 67 (11) (2024) 3499–3512.
[16] L.L. Fan, W.L. Dong, J.Q. Lu, Y.J. Peng, B. Xie, P. Wei, M. Jiang, S. Chen, Robust controlled degradation of enzyme loaded PCL-based fibrous scaffolds toward scarless skin tissue regeneration, *Adv. Sci.* 12 (25) (2025) 2501053.
[17] A. Almasi-Jaf, A. Shamloo, H. Shaygani, S. Seifi, Fabrication of heparinized bi-layered vascular graft with PCL/PU/gelatin co-electrospun and chitosan/silk fibroin/gelatin freeze-dried hydrogel for improved endothelialization and enhanced mechanical properties, *Int. J. Biol. Macromol.* 253 (Pt 2) (2023) 126807.
[18] S.Y. Zhou, L. Li, E. Xie, M.X. Li, J.H. Cao, X.B. Yang, D.Y. Wu, Small-diameter PCL/PU vascular graft modified with heparin-aspirin compound for preventing the occurrence of acute thrombosis, *Int. J. Biol. Macromol.* 249 (2023) 126058.
[19] M. Irani, G. Mir Mohamad Sadeghi, I. Haririan, A novel biocompatible drug delivery system of chitosan/temozolomide nanoparticles loaded PCL-PU nanofibers for sustained delivery of temozolomide, *Int. J. Biol. Macromol.* 97 (2017) 744–751.
[20] W. Ali, H. Jeong, J.S. Lee, P. Zinck, S. Souissi, Biodegradable microplastics interaction with pollutants and their potentialtoxicity for aquatic biota: a review, *Environ. Chem. Lett.* 22 (3) (2024) 1185–1220.
[21] C.W. Tang, L. Wang, J. Sun, G.D. Chen, J.F. Shen, L. Wang, Y. Han, J.R. Luo, Z.Y. Li, P. Zhang, S.M. Zeng, D.P. Qi, J. Geng, J. Liu, Z.J. Dai, Degradable living plastics programmed by engineered spores, *Nat. Chem. Biol.* 21 (7) (2025) 1006–1011.
[22] I. Khan, R. Nagarjuna, J.R. Dutta, R. Ganesan, Enzyme-embedded degradation of poly(ε-caprolactone) using lipase-derived from probiotic lactobacillus plantarum, *ACS Omega* 4 (2) (2019) 2844–2852.
[23] C. DelRe, Y.F. Jiang, P. Kang, J. Kwon, A. Hall, I. Jayapurna, Z.Y. Ruan, L. Ma, K. Zolkin, T. Li, C.D. Scown, R.O. Ritchie, T.P. Russell, T. Xu, Near-complete depolymerization of polyesters with nano-dispersed enzymes, *Nature* 592 (7855) (2021) 558–563.
[24] A.F. Greene, A. Vaidya, C. Collet, K.R. Wade, M. Patel, M. Gaugler, M. West, M. Petcu, K. Parker, 3D-printed enzyme-embedded plastics, *Biomacromolecules* 22 (5) (2021) 1999–2009.
[25] B. Panganiban, B.F. Qiao, T. Jiang, C. DelRe, M.M. Obadia, T.D. Nguyen, A.A.A. Smith, A. Hall, I. Sit, M.G. Crosby, P.B. Dennis, E. Drockenmuller, M. Olvera de

la Cruz, T. Xu, Random heteropolymers preserve protein function in foreign environments, *Science* 359 (6381) (2018) 1239–1243.
[26] D.X. Han, X.C. Wang, S.H. Song, H.Q. Shen, Y. Lu, Z.Z. Zheng, X.Q. Wang, Z.F. Han, G. Li, Advances in multifunctional medical sutures for wound healing: a review, *Colloids Surf. B Biointerfaces* 256 (Pt 2) (2025) 115062.
[27] X.C. Wang, H.Q. Shen, D.H. Shou, Y. Liu, T.Y. Wang, Z.Z. Zheng, Z.Y. Zhao, X. Q. Wang, G. Li, A braided surgical silk suture with controllable biodegradability *via* enzymatic hydrolysis, *Polym. Degrad. Stabil.* 230 (2024) 111080.
[28] A. Magnin, E. Pollet, R. Perrin, C. Ullmann, C. Persillon, V. Phalip, L. Avérous, Enzymatic recycling of thermoplastic polyurethanes: synergistic effect of an esterase and an amidase and recovery of building blocks, *Waste Manag.* 85 (2019) 141–150.
[29] J.W. Liu, Q.Y. Zeng, H.R. Lei, K.Y. Xin, A.M. Xu, R. Wei, D. Li, J. Zhou, W.L. Dong, M. Jiang, Biodegradation of polyester polyurethane by Cladosporium·sp. P7: evaluating its degradation capacity and metabolic pathways, *J. Hazard. Mater.* 448 (2023) 130776.
[30] A.U. Svensby, E. Nygren, A. Gefen, B. Cullen, Å.M. Ronkvist, A. Gergely, M.D. Craig, The importance of the simulated wound fluid composition and properties in the determination of the fluid handling performance of wound dressings, *Int. Wound J.* 21 (5) (2024) e14861.
[31] F. Santos-Beneit, L.M. Chen, S. Bordel, R. Frutos de la Flor, O. García-Depraect, R. Lebrero, S. Rodriguez-Vega, R. Muñoz, R.A. Börner, T. Börner, Screening enzymes that can depolymerize commercial biodegradable polymers: heterologous expression of fusarium·solani cutinase in escherichia coli, *Microorganisms* 11 (2) (2023) 328.
[32] N. Van Noten, E. Van Liefferinge, J. Degroote, S. De Smet, T. Desmet, J. Michiels, Fate of thymol and its monoglucosides in the gastrointestinal tract of piglets, *ACS Omega* 5 (10) (2020) 5241–5248.
[33] F. Kahvand, M. Fasihi, Plasticizing and anti-plasticizing effects of polyvinyl alcohol in blend with thermoplastic starch, *Int. J. Biol. Macromol.* 140 (2019) 775–781.
[34] M.I. Peñas, A. Beloqui, A. Martínez de Ilarduya, S. Suttiruengwong, R. Hernández, A.J. Müller, Enzymatic degradation behavior of self-degradable lipase-embedded aliphatic and aromatic polyesters and their blends, *Biomacromolecules* 25 (7) (2024) 4030–4045.
[35] S.F. Karkan, R. Rahbarghazi, S. Davaran, L.S. Kaleybar, A.B. Khoshfetrat, M. Heidarzadeh, E. Zolali, A. Akbarzadeh, Electrospun polyurethane/poly (ϵ-caprolactone) nanofibers promoted the attachment and growth of human endothelial cells in static and dynamic culture conditions, *Microvasc. Res.* 133 (2021) 104073.
[36] J. Kim, G.G. Zhang, M. Shi, Z.G. Suo, Fracture, fatigue, and friction of polymers in which entanglements greatly outnumber cross-links, *Science* 374 (6564) (2021) 212–216.
[37] Z. Zarekhalili, S.H. Bahrami, M. Ranjbar-Mohammadi, P.B. Milan, Fabrication and characterization of PVA/Gum tragacanth/PCL hybrid nanofibrous scaffolds for skin substitutes, *Int. J. Biol. Macromol.* 94 (Pt A) (2017) 679–690.
[38] P. Paitaid, A. H-Kittikun, Enhancing immobilization of Aspergillus oryzae ST11 lipase on polyacrylonitrile nanofibrous membrane by bovine serum albumin and its application for biodiesel production, *Prep. Biochem. Biotechnol.* 51 (6) (2021) 536–549.
[39] S.C. Sebag, M.H. Hao, Q.W. Qian, C. Upara, Q. Ding, M. Zhu, J.A. Banas, H.J. Cao, L. Hong, L. Yang, A medium chain fatty acid, 6-hydroxyhexanoic acid (6-HHA), protects against obesity and insulin resistance, *Acta Pharm. Sin. B* 14 (4) (2024) 1892–1894.
[40] S.X. Chen, L.P. Ge, A. Mueller, M.A. Carlson, M.J. Teusink, F.D. Shuler, J.W. Xie, Twisting electrospun nanofiber fine strips into functional sutures for sustained co-delivery of gentamicin and silver, *Nanomedicine* 13 (4) (2017) 1435–1445.
[41] J.Y. Hu, Y. Song, C.Y. Zhang, W. Huang, A.Q. Chen, H.C. He, S.S. Zhang, Y.X. Chen, C.D. Tu, J.H. Liu, X. Xuan, Y. Chang, J. Zheng, J. Wu, Highly aligned electrospun collagen/polycaprolactone surgical sutures with sustained release of growth factors for wound regeneration, *ACS Appl. Bio Mater.* 3 (2) (2020) 965–976.
[42] Y.L. Cui, Y.C. Chen, J.Y. Sun, T. Zhu, H. Pang, C.L. Li, W.C. Geng, B. Wu, Computational redesign of a hydrolase for nearly complete PET depolymerization at industrially relevant high-solids loading, *Nat. Commun.* 15 (1) (2024) 1417.